Convective heat transfer for cold tube bundles with ice formations in a stream of water at steady state

Paul Alexander Intemann and Michael Kazmierczak
Department of Mechanical, Industrial and Nuclear Engineering, University of Cincinnati, Cincinnati, OH, USA

Experiments were conducted on cold-tube banks subjected to a cross-flow of water. The tubes were internally cooled below the freezing temperature and became enveloped in ice. The resulting ice shapes, which formed on the outside surfaces of the tubes, were allowed to stabilize, and their impact on the total steady-state rate of energy exchange between the tubes and the flowing water was investigated.

Both in-line and staggered tube-bank geometries were considered, with tests conducted in the low to moderate Reynolds number range ($Re_d = 100$–$2{,}000$) and for cooling-temperature ratio variations of $0.5 < \Theta < 8$. The ice formations were directly observed and photographed, and the total heat transfer rate for the tube bank was inferred from a simple energy balance on the system.

The ice shapes that formed around the tubes were described by one of three distinct categories: ice formations with no linkage occurring between any adjacent tubes; ice formations with partial linkage of some adjacent tubes; and, for the staggered tube bank, a complete linkage of a majority of the tubes.

The experiments showed that the ice formations dramatically affected the convective heat transfer rate of the tube banks (when compared to nonicing tube banks at the same Re_d) and that the change in heat transfer rate is dependent on the tube-bank geometry. In the no-link category, the ice formations were found to either increase or decrease the tube-bank heat transfer rate depending on the amount of ice-build accumulation, the staggered configuration showing a greater overall rise with Θ than the in-line geometry. Ice linkage between adjacent tubes was found to be detrimental to the heat transfer rate of the staggered bank; however, the same phenomenon on the in-line tube bank did not seriously impede its heat transfer rate. Correlations expressing the heat transfer behavior of both in-line and staggered tube banks with ice formations at steady state have been developed.

Keywords: phase-change phenomena; forced convection; thermal energy storage

Introduction

The phenomenon of forced convective freezing of ice in a tube-bank geometry has only recently received the attention of the scientific research community, primarily due to the increased interest in commercially viable phase-change thermal-energy storage systems. While studies of fluid flow and heat transfer by tube banks without phase change, as well as research into melting and freezing heat transfer in general, have been reported by the research community, the simultaneous occurrence of both phenomena has only recently been explored by a small group of investigators.

The heavy reliance on tube-bundle heat exchangers in many industrial applications was partially responsible for the upsurge in research activities concerning tube-bank fluid flow and heat transfer characteristics that occurred during the 1950s and continued unabated into the 1970s. Due to the well-documented flow complexities associated with flow through tube bundles, such as flow separation and nonuniform tube heat transfer film coefficients, most of the studies to date and the design data generated from these studies have arisen from experimental investigations. The most thorough and complete study of the experimental heat transfer and fluid flow characteristics exhibited by tube banks in cross-flow is found in Zukauskas and Ulinskas (1988).

In contrast, solid–liquid phase-change heat transfer, also known as melting and freezing heat transfer, is a research area that historically enjoyed a rather rich yet generally unnoticed tradition in the open literature, but which, due to the energy crisis during the early 1970s, has exploded during the past two decades. The majority of these studies were concerned with conduction-dominated phase-change heat transfer and, in general, dealt with convective solidification problems in a much more limited sense by considering only very simple flow fields and geometries—conditions exactly opposite to those that exist in a tube-bank flow field. As many researchers investigating these simple flow fields have discovered, under certain situations, the interaction between the solid–liquid interface and the surrounding flow field may become sufficiently strong that only a coupled solution to the problem would yield reasonable results (Hirata et al. 1979; Gilpin et al. 1980). The problem investigated in this paper is one such case in which

Address reprint requests to Professor Kazmierczak at the Department of Mechanical, Industrial and Nuclear Engineering, University of Cincinnati, OH 45221-0072, USA.

Received 13 April 1994; accepted 14 July 1994

the mutual dependence between the interface and the flow field must be taken into account. For a thorough discussion on flow-freezing interactions found in convective solid–liquid phase-change problems, the reader is referred to the excellent review article of Cheung and Epstein (1984).

As far as we have been able to determine, only a very limited number of published studies exist that investigate the phenomenon of forced convective freezing of ice on anything resembling a tube-bank geometry. While many studies focusing on single or dual cylinder arrangements in a cross-flow have been reported (Okada et al. 1978; Cheng et al. 1981; Lock and Kaiser 1985), the very first investigators to explore the ice formation of staggered cooled cylinders in a water cross-flow were Okada et al. (1987). This study was followed by that of Hirata and Matsui (1990), who investigated the ice-formation phenomena around a single line of isothermally cooled cylinders. Next, Torikoshi and Nakazawa (1990, 1992) investigated the formation of ice around horizontally mounted tubes in both in-line and staggered arrangements, but all their freezing experiments were conducted with the tubes immersed in a stagnant water bath without any externally imposed cross-flow occurring past the tubes. Most recently, Hirata and Matsui (1992) released a study reporting on the freezing heat transfer with water flow around isothermally cooled cylinders in both staggered and aligned arrangements. Even though the cylinder arrangements used by Hirata and Matsui (1992) were in effect a single line of tubes, flanked on either side by semicylindrical tubes attached to the test-facility tunnel bounding walls, and therefore not exactly a full-fledged tube-bank design, the study represents the latest and therefore perhaps the best attempt to date to look at the forced convective freezing of an experimental configuration that is similar in design to a "real-world" tube-bank heat exchanger.

The steady-state experiments presented in this study significantly expand the existing database and, for the first time, document the heat transfer rate of both a staggered and an in-line multirow, multicolumn tube bank in a cross-flow of water with ice formation. The trends observed are expressed in empirical correlations similar in form to those developed by Zukauskas and Ulinskas (1988), but include the dimensionless cooling temperature ratio Θ as a new, additional parameter.

Experimental apparatus

All experiments were performed in the University of Cincinnati Experimental Freezing/Melting Water Tunnel shown schematically in Figure 1. An actual photo layout of the test facility is shown in Figures 2 to 4. The experimental setup as outlined in Figure 1 consisted of four major subsystems: the water tunnel and its flow control, the test section, the cooled tube bank, and the data acquisition and process control equipment.

Water tunnel and flow control

The main body was constructed primarily of 1.91-cm-thick clear Plexiglas and, in areas where fluid observation was deemed nonessential, was assembled using schedule 80-PVC piping and fittings. The major subassemblies of the tunnel consisted of the following:

- a 3-hp variable-speed centrifugal water pump with a design speed of 3,600 RPM connected to a digital electronic control device. The electronic control unit was capable of setting the pump speed to any constant RPM value required by the operator; for the experiments reported in this study, the flow rates ranged from 0.9 to 14.8 m^3/hr (4 to 65 GPM);

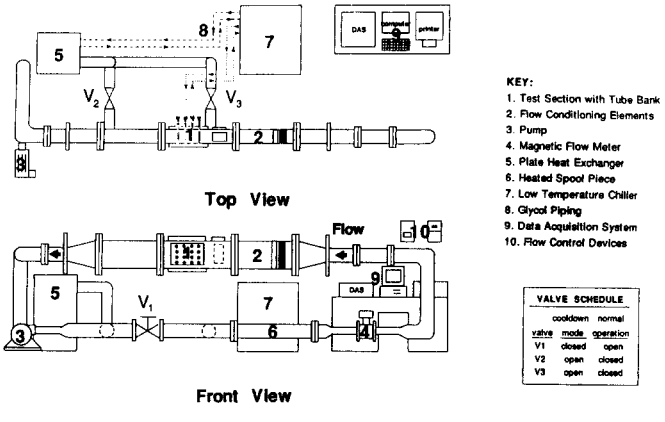

Figure 1 Sketch of freezing/melting water tunnel

Notation

A	Tube bank total exterior surface area, cm^2
AR	Aspect ratio of tube bank, h/l
cl	Correction factor for short-tube-bank heat transfer calculation
d	Tube outside diameter, cm
h	Vertical distance between adjacent tubes, cm
k	Thermal conductivity, W/m – K
K	Heat transfer parameter, Equation 5
l	Horizontal distance between adjacent columns of tube, cm
Nu	Average experimental Nusselt number, Equation 4
Pr	Prandtl number, ν/α
Q	Heat transfer rate, W
Re	Reynolds number, Equation 2
T	Temperature, K
V	Velocity, cm/s
W	Work, W

Greek symbols

α	Thermal diffusivity, cm^2/s
Θ	Cooling-temperature ratio, Equation 3
μ	Dynamic viscosity, g/cm – s
ν	Kinematic viscosity, cm^2/s
ρ	Fluid density, g/cm^3

Subscripts

bank	Tube bank
c	Parameter corrected for short-tube-bank data
d	Tube exterior diameter
f	Fluid (water)
i	Ice/water interface
max	Maximum
pump	Centrifugal water pump
spool	Heated spool piece
system	Water tunnel
w	Tube wall
∞	Freestream condition

Superscript

—	Denotes quantity is average of all tubes

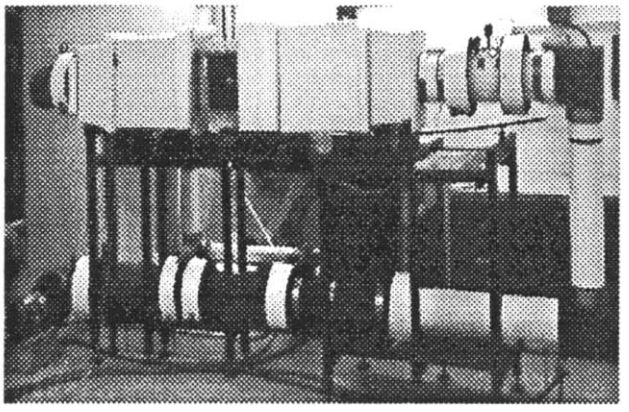

Figure 2 Freezing/melting water tunnel

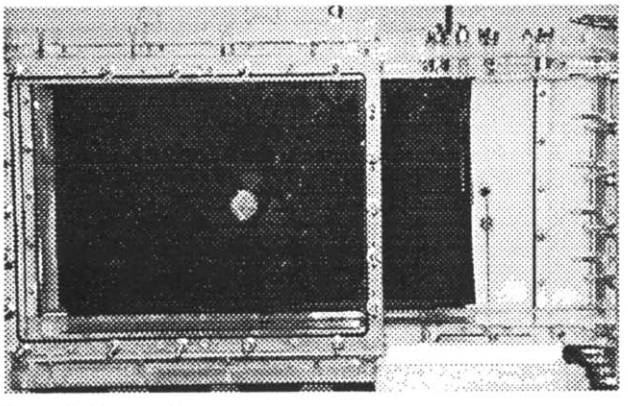

Figure 3 Test section

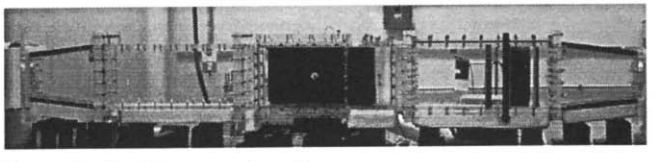

Figure 4 Plexiglas tunnel sections

- a magnetic flowmeter device, used to measure the tunnel's water flow rates with an accuracy of ± 1.0 percent of the indicated flow rate;
- a flow conditioning section located upstream of the test section, used to ensure a uniform flow distribution at the test section inlet. It consisted of a diffuser vane, two baffle plates, polyfoam material, and a honeycomb flow straightener. This configuration was found to yield acceptable vertical and horizontal velocity profiles, as confirmed by hydrogen bubble flow visualization, at the tube-bank inlet; and
- a plate heat exchanger, a high-capacity low-temperature chiller, and a heated spool piece, collectively utilized to accurately control the tunnel water temperature. The chiller and plate heat exchanger were used during the initial tunnel cool-down period, when the water was brought from an ambient room temperature down to a near-freezing temperature in a matter of hours. The heat exchanger was then valved out of the system (see Figure 1 valve schedule), and the chiller was then piped to supply the tube bank with a 50–50 glycol–water mixture to begin the ice-making process. The energy extraction of the tube bank was usually greater than the combined system energy gain through the tunnel walls and the pump work, so a heated spool piece was added to the configuration to maintain a constant temperature of the water entering the test section. Active control of the heated spool piece was automated by means of a digital PID temperature controller that measured the tube-bank inlet water temperature, compared it to the required setpoint temperature, and automatically varied the power to the spool-piece section to maintain the aforementioned setpoint temperature within ± 0.1°C.

Tunnel test section

The actual freezing of water was initiated and took place on the cold tube banks that were inserted inside the test section. The dimensions of the test section where the solidification occurred measured 25.4 cm high by 12.7 cm deep by 38.1 cm long. Figure 3 shows the test section and, clearly visible, the two (front and rear) large removable test windows that were used to hold the tubes in place. Two different sets of windows, one with a staggered hole arrangement and one with an in-line arrangement, were machined to study the effects of the tube placement on the ice formation process. The exact tube-bank dimensions used in the present study are shown in Figures 5 and 6. The test-section walls were manufactured using double-layered Plexiglas plates in order both to reduce the heat

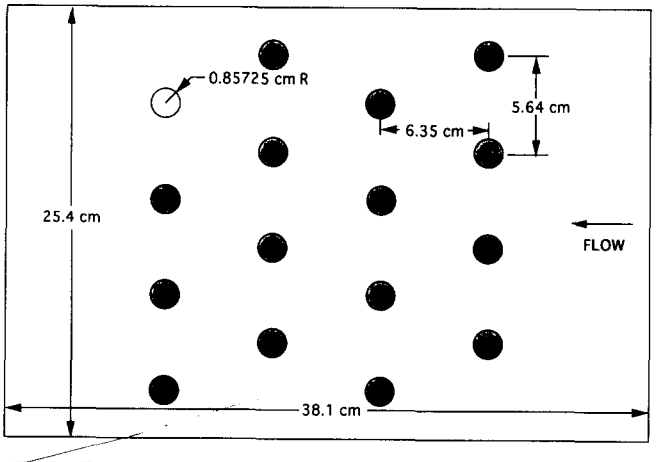

Figure 5 Staggered tube-bank arrangement showing dimensions

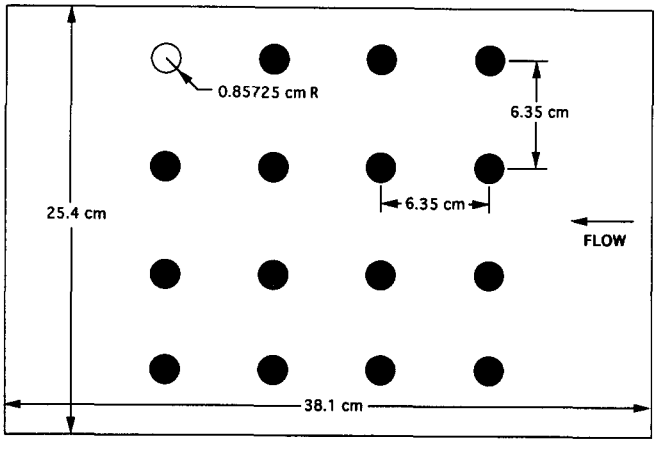

Figure 6 In-line tube-bank arrangement showing dimensions

gain into the test section through the windows and to prevent unwanted condensation on the exterior surfaces.

Tube banks and tubes

Both of the tube banks that were tested consisted of 16 identical tubes. These were all cooled internally, in parallel, to below the fusion temperature of water with a 50–50 glycol and water mixture supplied by the low-temperature chiller. Coolant entry into and exit out of the tubes was located on the same side of the tunnel to permit unimpeded viewing of the tube bank and ice formations during the experiments. A schematic layout of the test tube architecture is given in Figure 7. Once the water–glycol mixture entered the coolant reservoir, it proceeded down the thin-walled inner center tube, exited that tube through a series of small radial end holes, and returned back to the reservoir via the annulus formed by the inner tube and the copper pipe on whose exterior the ice formations occurred. All the tubes were manufactured using commercially available thick-walled copper pipe. In order to obtain the tube wall temperature and to verify the isothermal condition of the copper pipe, three type-T thermocouples, evenly spaced along the length, were imbedded in the surface of each tube.

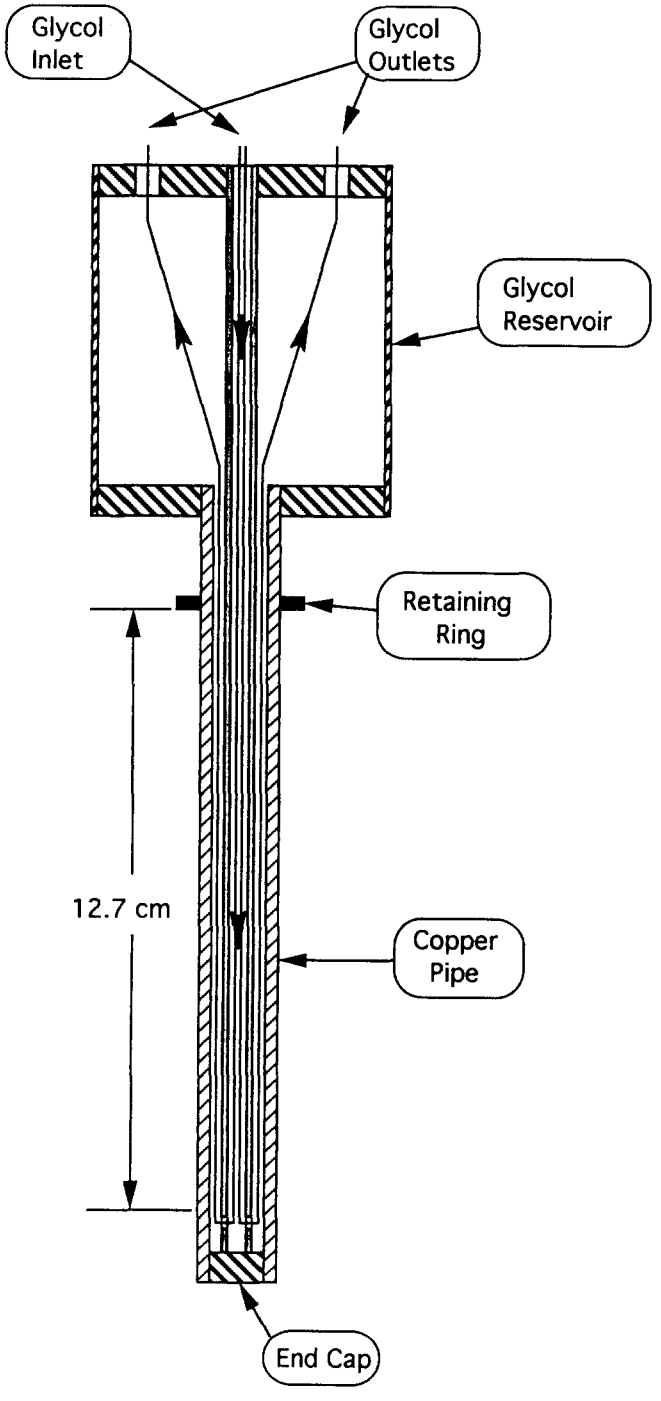

Figure 7 Tube cut-away view

Tube bank heat transfer rate

The heat transfer rate Q_{bank} through the ice-covered tube bank was calculated using a relatively simple form of energy balance on the flowing water. It included the work added to the system by the water pump W_{pump}, which was calculated from known pump-pressure rise and efficiency information, and the energy added to the water via the heated spool piece Q_{spool}. The final term needed in the energy balance equation was the heat gain of the system due to the environmental imbalances between the water temperature and the test-facility room temperature. This Q_{system} was determined prior to collecting any freezing data by elevating the tunnel water temperature, by means of the heated spool piece, above the ambient room temperature and, knowing W_{pump} and Q_{spool} with Q_{bank} equal to zero, simply calculating the Q_{system} value once the system had attained steady state. This procedure was repeated for a range of ΔT's between the water and the room, and resulted in a linear relation for Q_{system} with temperature difference. With this information, the steady-state tube-bank heat transfer rate was then calculated as follows:

$$Q_{bank} = Q_{system} + Q_{spool} + W_{pump} \quad (1)$$

Data acquisition and process control

All measurements and data collection were done using an HP 75000 data acquisition system in conjunction with an HP Vectra 386/20 computer running LabTech Notebook software. A closed single-loop feedback control algorithm was implemented using the computer software and the data acquisition hardware that incrementally increased the centrifugal pump speed to maintain constant volumetric flow, thereby correcting for changes in flow resistance brought about by test-section constrictions due to large ice buildup on the tube banks. In addition, the system also continuously monitored the heater PID controller output signal and, from this information, calculated the energy added to the system by the heated spool piece. All temperatures (tube wall, water, and glycol circuits), flow rate, spool-piece wattage, and pump speed were automatically scanned and recorded by the data acquisition system and saved on the hard disk of the PC.

Experimental procedure and data reduction

All steady-state experiments followed essentially the same basic procedure. Initially, the plate heat exchanger was valved into the system and, once the low-temperature chiller had reached an adequately low glycol–water temperature, the tunnel water temperature was lowered until it was approximately 2 to 3°C. This typically took anywhere from 1 to 2 hours. Once this was accomplished, the plate heat exchanger was valved out, and the chiller glycol–water temperature was reset to a new value. This new, chiller-set temperature was determined based upon the desired cooling temperature ratio Θ of the current test. Once

this new value was achieved, the glycol–water mixture was then circulated through the tube bank to cool the tubes and to begin the freezing process. Initially the ice grew rapidly, but growth slowed significantly with time. Eventually, when $Q_{conduction}$ equalled $Q_{convection}$ at the ice–water interface, the ice growth stopped and steady-state conditions prevailed. The length of time it took for the system to achieve a steady-state condition varied somewhat depending on imposed test conditions, but in general 12 to 18 hours were usually sufficient to allow the system to stabilize. Once steady-state was achieved, the data were logged by the data acquisition system. These data were then reduced using a spreadsheet program that calculated the following: the Reynolds number Re_f based on the freestream conditions and maximum fluid velocity through the tube bank, the value of the cooling temperature ratio Θ, which is a measure of the degree of ice subcooling compared to the cross-flow water superheating, and the tube-bank average Nusselt number $\overline{Nu_f}$ for each experimental run:

$$Re_f = \frac{\rho V_{max} d}{\mu} \tag{2}$$

$$\Theta = \frac{(T_i - T_w)}{(T_\infty - T_i)} \tag{3}$$

$$\overline{Nu_f} = \frac{Q_{bank} \times d}{kA(T_\infty - T_i)} \tag{4}$$

In addition, the program also calculated the $\overline{K_f}$ factor, a modified form of the Nusselt number with the Prandtl number dependence eliminated, as defined below:

$$\overline{K_f} = \frac{\overline{Nu_f}}{Pr_f^{0.36}(Pr_f/Pr_i)^{0.25}} \tag{5}$$

where the assumed values of the exponents are the accepted empirically derived constants from the work of Zukauskas and Ulinskas (1988).

Finally, all fluid property values such as density, viscosity, and thermal conductivity, as well as the Prandtl numbers were calculated by the program using table curve look-up routines evaluated at the test-conditions free-stream water temperature.

Uncertainty analysis

The procedure presented by Moffat (1988) and applicable to single-sample experimental data collection/reduction was implemented to obtain a measure of the uncertainty in the reported results for Re_f and $\overline{K_f}$. The typical uncertainty associated with the Reynolds number and $\overline{K_f}$, spanning all 63 experimental data points collected, was determined to be approximately 1.3 percent and 6.2 percent, respectively. The maximum uncertainty in $\overline{K_f}$ (Experiment 38) was found to be 9.32 percent. Likewise, the typical uncertainty in $\overline{K_f}$ for the tube-bank heat transfer validation runs was found to be approximately 4.1 percent, with a maximum uncertainty of 5.16 percent. Note that these results include both bias and random errors of the measured variables. The possible sources of error in the reported Reynolds numbers included the water flow-velocity uncertainty, the tube-diameter measurement accuracy, and the inherent "fossilized" error in the reference water viscosity. The uncertainty in $\overline{K_f}$ arises from the possible errors in the numerous variables used in calculating its final value, starting from the required measurements needed for the evaluation of the various terms in the energy balance. Heated-spool-piece supply voltage fluctuations, thermocouple accuracy uncertainties, environmental heat-gain calibration-curve fit accuracy, and "fossilized" errors in fluid properties are examples of some of the potentially larger sources of errors that were considered in the analysis.

Tube-bank heat transfer validation runs

Before performing any freezing tube-bank experiments, it was necessary to first verify the accuracy of the method used to measure the tube-bank heat transfer rate as outlined above. A series of nonicing experiments were therefore conducted in which our measured rate of heat transfer was compared to the classical results obtained by Zukauskas and Ulinskas (1988). Since our data were collected using a four-column tube bank, and since the reported correlations apply to tube banks with 20 or more columns, the $\overline{Nu_f}$ and $\overline{K_f}$ values obtained were appropriately adjusted using the Zukauskas and Ulinskas (1988) factors for short tube banks as shown below:

$$Nu_{fc} = c1 \times \overline{Nu_f} \tag{6}$$

$$K_{fc} = c1 \times \overline{K_f} \tag{7}$$

where c1's for four-column tube banks are determined to be

c1 = 1.00 for $Re_f < 1{,}000$ and c1 = 0.91 for $Re_f > 1{,}000$ for in-line tube banks

c1 = 0.94 for $Re_f < 1{,}000$ and c1 = 0.90 for $Re_f > 1{,}000$ for staggered tube banks

Comparison of our test data with the standard correlations developed by Zukauskas and Ulinskas (1988) (displayed at the top of Figures 8 and 9) shows very good agreement for both geometries of interest. It is interesting to note that, since our test data span the Reynolds number range of 1,000, a value at which the correlation changes, we find that our data for the staggered arrangement (Figure 8) display the expected change in slope, but the data for the in-line arrangement rather appear to be "sandwiched somewhere between" the two respective correlations listed in Figure 9. Regardless of this subtle difference between the two figures and our data, it is concluded that, due to the relatively close agreement between the validation-run results and these well-accepted correlations, the system energy balance method described earlier is a reasonably accurate and experimentally acceptable method to use for finding Q_{bank}.

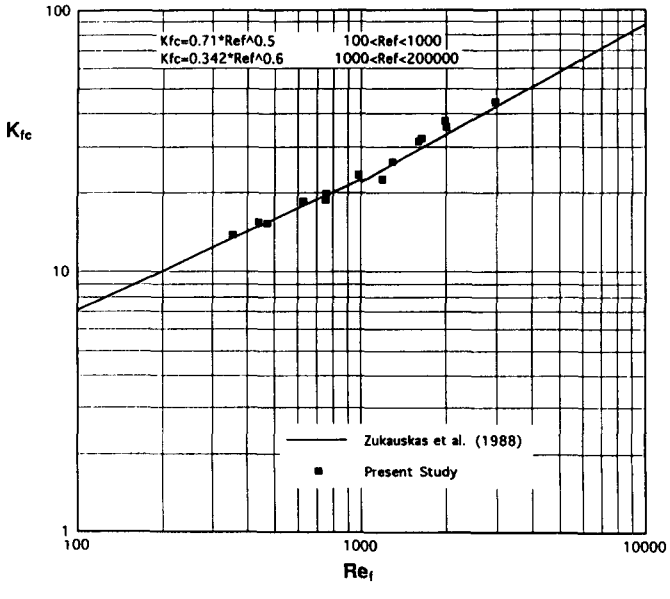

Figure 8 Staggered nonfreezing tube-bank heat transfer validation experiments

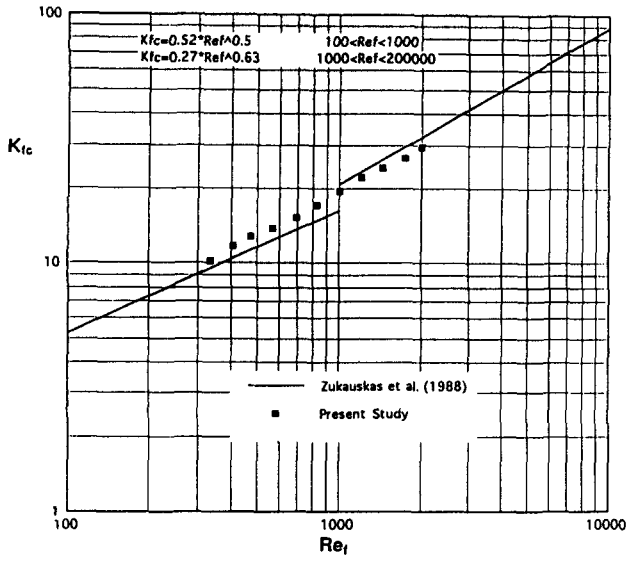

Figure 9 In-line nonfreezing tube-bank heat transfer validation experiments

Results and discussion

Staggered tube bank

A total of 40 steady-state experiments were performed using the staggered tube bank, in which the Reynolds number and the dimensionless cooling temperature ratio Θ were varied from 170 to 1,750 and 0.5 to 8, respectively. Results of these runs, for which K_{fc} (fifth column of Table 1) was calculated according to Equation 5, are reported in Table 1. While the differences in the heat transfer between our experimental results obtained with ice formations and those reported by Zukauskas and Ulinskas (1988) for a clean tube bank without ice can be rather significant (sixth column of Table 1), an interesting trend develops when the results are plotted as shown in Figure 10. It appears that the tube-bank heat transfer with ice buildup is less than the nonicing tube-bank heat transfer (dashed line in Figure 10) when the dimensionless cooling temperature ratio is less than 1—and for larger Re_f experiments, in some cases when Θ is less than 2—but becomes significantly larger than a nonicing tube bank when the ratio is 4 and above. It is interesting to note that two experiments, runs 17 and 22 (Table 1), resulted in partial ice bridging between adjacent tubes and

Table 1 Summary of staggered freezing tube-bank results

Run	Re_f	Θ	$\overline{Nu_f}$ (Eq. 4)	K_{fc} (experiments)	% Difference[a] vs. Zukauskas correlation	% Difference[b] vs. Eq. 8 correlation
1	671	3.83	55.96	24.79	34.78	5.92
2	670	2.10	41.56	18.41	0.17	−7.10
3	661	1.12	34.64	15.20	−16.74	−8.32
4	664	0.55	31.94	14.08	−23.03	9.28
5	663	4.14	58.85	26.02	42.31	9.28
6	664	7.99	73.73	31.89	74.34	11.60
7	964	8.11	70.90	30.66	39.10	−6.60
8	1004	7.57	66.82	30.96	39.87	−5.27
9	1010	3.96	54.71	25.70	15.69	−6.16
10	995	1.99	47.96	21.39	−4.52	−4.95
11	1000	1.05	40.11	17.90	−20.28	−5.20
12	1005	0.53	34.96	16.70	−24.60	6.77
13	430	2.00	37.53	16.43	11.56	−1.35
14	438	1.04	32.61	14.40	−6.08	2.65
15	439	0.53	28.26	12.48	−16.07	7.59
16	438	8.48	69.35	30.00	101.97	20.00
17	437	8.30	62.89	27.21	83.32	9.53
18	293	1.88	27.74	12.21	0.36	−14.49
19	306	4.21	44.95	19.86	59.81	9.65
20	302	1.10	25.04	11.08	−10.16	−10.78
21	301	0.48	22.80	10.18	−17.28	3.27
22	298	8.26	58.54	25.29	106.42	17.07
23	1298	3.68	52.60	24.95	−3.38	−15.00
24	1322	2.06	45.31	21.65	−17.09	−14.08
25	1298	1.04	39.79	19.13	−25.93	−7.07
26	1325	0.51	38.45	18.59	−28.93	8.34
27	1745	1.65	54.14	26.43	−14.31	1.05
28	664	8.35	65.19	28.17	53.97	−2.63
29	691	4.14	52.32	23.11	23.85	−4.39
30	1009	4.31	52.85	24.77	11.58	−11.57
31	1014	7.99	71.50	33.14	48.88	−0.45
32	1674	0.99	50.57	24.79	−17.58	10.66
33	1733	0.51	49.30	24.30	−20.89	29.08
34	172	2.06	27.83	12.42	33.26	2.47
35	171	4.06	35.43	15.55	67.34	6.93
36	173	1.09	20.87	9.34	−0.11	−7.88
37	176	5.55	20.70	9.26	−1.64	Not included
38	176	0.50	18.29	8.21	−12.73	−0.05
39	170	1.05	20.10	9.00	−2.70	−9.27
40	299	1.95	31.39	13.82	12.56	−4.69

[a] $[(K_{fc}$ (experimental) $- K_{fc}$ (Zukauskas and Ulinskas)$)/K_{fc}$ (Zukauskas and Ulinskas)$] \times 100$.
[b] $[(K_{fc}$ (experimental) $- K_{fc}$ (Eq. 8)$)/K_{fc}$ (Eq. 8)$] \times 100$.

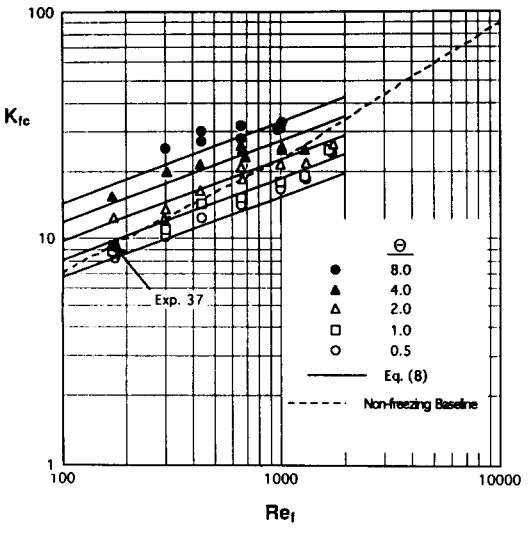

Figure 10 Staggered freezing tube-bank heat transfer results

that one run, Experiment 37, resulted in a steady-state configuration in which 13 of the 16 tubes were completely connected. Figure 11a shows the ice shape for run 21 that represents the typical steady-state ice shapes (with no linkage) found in the majority of runs, while Figure 11b shows the case of almost complete linkage of run 37. Experiment 37 has been highlighted on Figure 10 and clearly shows that significant ice bridging between adjacent tubes, generally occurring at lower Re_f and higher Θ values, is detrimental to the overall heat removal rate of the tube bank.

While at first it may seem surprising to the casual observer that the heat transfer of an ice-on-tube-bank design should exhibit the behavior shown in Figure 10, the explanation for the *increase* of K_{fc} *above* the nonfreezing baseline data may be relatively simple. If the tube bank were tested at $\Theta = 0$, one would expect the resulting data points in Figure 10 to fall somewhere very close to the dashed, nonfreezing baseline. As Θ is increased and more ice forms on the exterior surface of the tubes, the ice surface area exposed to convection becomes much larger. Also, the increase in flow velocity (and turbulence) within the tube bank due to the thicker ice layers at higher values of Θ is another influencing factor. These two combined effects, we feel, are responsible for increasing the overall tube-bank heat transfer rate beyond that of a nonicing tube bank of the same geometry, at elevated cooling temperature ratios. It is worth reporting that a similar trend was previously reported by Cheng et al. (1981), who earlier studied steady-state convection from a *single* tube with ice formation in a cross-flow of water. While a quantitative comparison between the results generated in this study and the previously published experimental works is not possible, due to the inherent differences in test configurations, it is nonetheless interesting to note that the work with a single tube revealed the same overall trend, when varying Reynolds number and Θ, in the reported heat transfer rate: i.e., the heat transfer was enhanced, and its magnitude increased with Θ. Now on the other hand, the reasons responsible for the *reduction* of K_{fc} *below* the nonfreezing baseline results (dashed line of Figure 10) are not yet clear. Data analysis to determine the local convective heat transfer coefficient at the ice–water interface of each tube is currently under way to help explain the unexpectedly low values of K_{fc} found to occur at Θ values less than 1 (and for larger Re_f experiments, in some cases Θ values less than 2), and will be reported at a later time.

The experimental data points shown in Figure 10 were statistically analyzed to determine a correlating equation that describes the experimental steady-state data. Judging from the data trends observed, an equation similar to that of Zukauskas and Ulinskas (1988) was expected and tried, but with the obvious inclusion of the Θ parameter. The best equation to date, with the least error, that has been generated to fit the measured data of this study is the correlation shown below:

$$K_{fc} = 1.545 \times Re_f^{0.361} \times \Theta^{0.277} \quad (8)$$

This equation is plotted as the solid lines in Figure 10 for five different Θ values and shows the correct general behavior with fair to good agreement with each experimental test. The point-by-point deviation from this new correlation is tabulated in the very last column of Table 1 with the multiple coefficient of determination R^2 being 0.94.

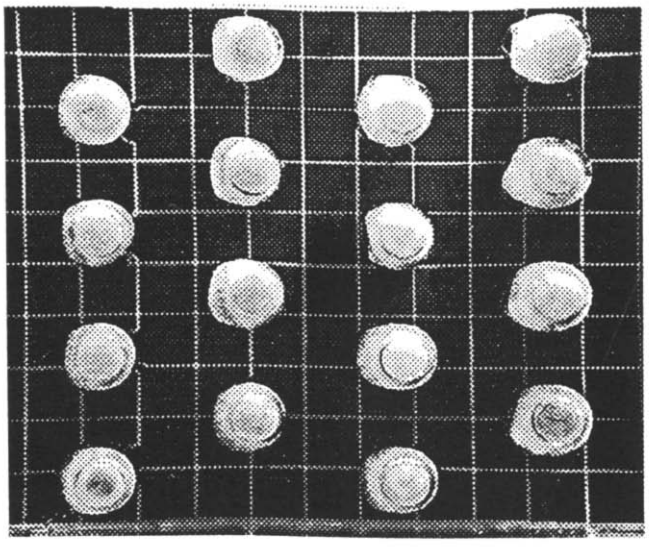

(a)

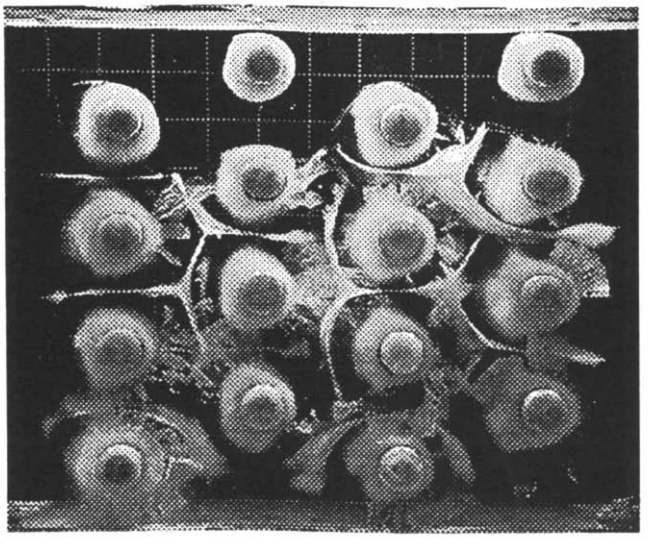

(b)

Figure 11 Staggered tube-bank ice shapes. (a) Run 21, a typical experiment with isolated ice shapes; (b) Run 37, a majority of the tubes connected due to ice bridging

In-line tube bank

Following the conclusion of the data runs utilizing the staggered tube bank arrangement, the in-line tube bank was installed in the water tunnel and a total of 23 steady-state experiments were conducted. While the range of cooling temperature ratios was the same as for the staggered tube-bank experiments, the Reynolds number range was reduced to only cover $Re_f = 170$ through 1,000 due to the lack of appreciable ice coating on the tubes at Reynolds numbers beyond 1,050. Table 2 is a summary of the results obtained for the in-line tube bank using the appropriate Pr dependence in defining K_{fc} for in-line tube banks. The data again show a significant difference in heat transfer when compared to the case without ice (Table 2, sixth column), although this deviation is now smaller in magnitude than the results previously obtained for the staggered tube-bank arrangement. The data are plotted in Figure 12 and exhibit the same basic behavior as observed for the staggered bank array, i.e., K_{fc} increases with Θ, but is below the nonfreezing baseline for small Θ and above it for higher Θ. During the experiments it was noted that the adjacent tubes in the in-line tube-bank configuration were much more likely to connect via an ice bridge than adjacent tubes in the staggered tube-bank arrangement at comparable Re_f and Θ values. For example, in the in-line arrangement, 10 of the 23 runs had partial or total linking of one or more rows, as compared to only three experiments with ice linkage in the staggered arrangement. Figure 13 shows three representative examples of the in-line tube-bank ice shapes: without linkage (Figure 13a, run 8), separate linked rows (Figure 13b, run 7), and multiple linked rows that were connected (Figure 13c, run 9).

One explanation that could account for the greater affinity of the in-line tube bank to link may be found in the "shadowing" effect present in the in-line tube-bank arrangement, which is absent in the staggered arrangement. This effect increases when the ice-formation diameters on the first column

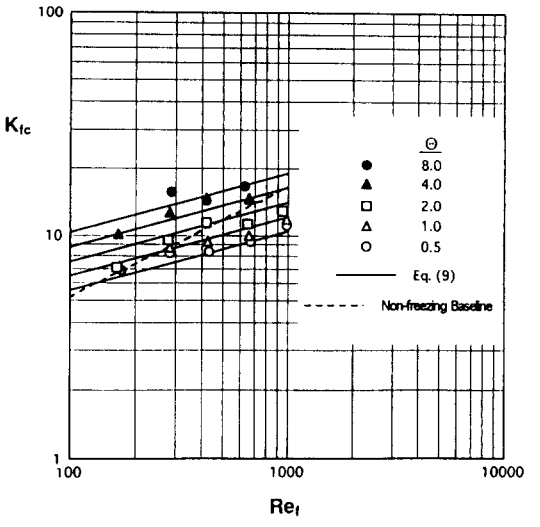

Figure 12 In-line freezing tube-bank heat transfer results

of tubes in the bank grow to the point where the downstream tubes are effectively blocked more and more from direct flow impingement by the water due to the increased upstream wake effects. As the ice diameters on the first column of tubes become larger, the downstream tubes in essence then sit in a region of even lower fluid velocities—a condition that, in turn, promotes even greater ice growth until adjacent tubes within the same row readily connect, as shown in Figure 13b. The variation of K_{fc} with Re_f and Θ for the in-line geometry is very similar to that exhibited by the staggered tube-bank arrangement and can be explained in a similar fashion as before, but with the following slight modification. While the "shadowing" effect of

Table 2 Summary of in-line freezing tube-bank results

Run	Re_f	Θ	$\overline{Nu_f}$ (Eq. 4)	K_{fc} (experiments)	% Difference[a] vs. Zukauskas correlation	% Difference[b] vs Eq. 9 correlation
1	414	2.01	27.41	11.39	7.55	2.76
2	424	0.98	22.05	9.28	−13.31	−2.86
3	429	0.47	19.82	8.39	−22.05	2.60
4	414	4.01	35.32	14.70	38.85	14.33
5	418	7.89	34.91	14.34	34.94	−3.72
6	288	8.42	38.23	15.68	77.73	14.73
7	165	4.03	24.29	10.08	50.74	0.35
8	658	3.93	35.19	14.64	9.72	0.98
9	632	6.07	40.49	16.69	27.66	6.00
10	172	0.50	16.29	6.91	1.30	6.65
11	169	0.97	16.95	7.17	6.20	−3.59
12	163	2.08	16.98	7.16	7.93	−17.47
13	284	0.50	19.76	8.28	−5.60	11.44
14	285	1.00	21.18	8.85	0.87	2.67
15	282	1.96	22.95	9.55	9.45	−3.80
16	286	3.94	30.27	12.57	43.05	−3.91
17	665	1.00	23.37	9.93	−25.93	−8.33
18	671	0.50	21.98	9.39	−30.30	0.44
19	650	2.01	26.63	11.22	−15.39	−10.32
20	943	1.97	29.77	12.86	−19.49	−6.61
21	977	0.98	26.80	11.73	−27.85	−2.01
22	989	0.51	25.13	11.05	−32.40	5.98
23	660	4.00	35.08	14.58	9.19	0.15

[a] $[(K_{fc}\text{ (experimental)} - K_{fc}\text{ (Zukauskas and Ulinskas)})/K_{fc}\text{ (Zukauskas and Ulinskas)}] \times 100$.
[b] $[(K_{fc}\text{ (experimental)} - K_{fc}\text{ (Eq. 9)})/K_{fc}\text{ (Eq. 9)}] \times 100$.

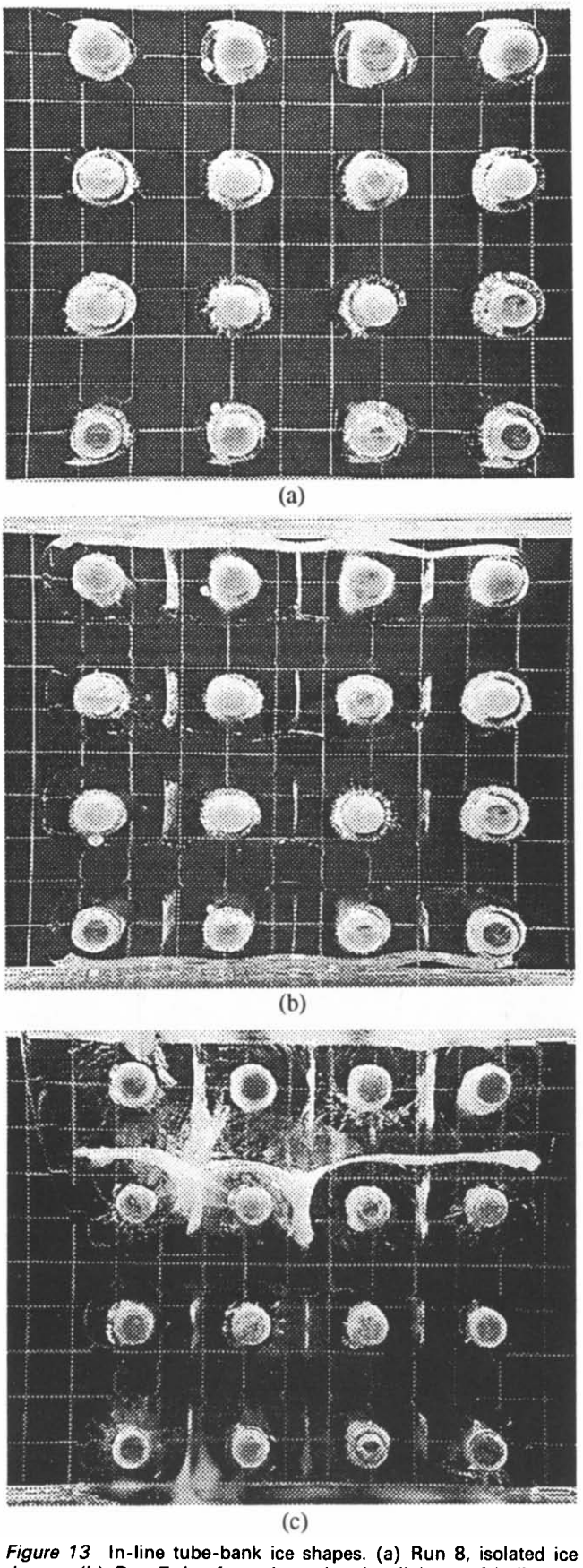

Figure 13 In-line tube-bank ice shapes. (a) Run 8, isolated ice shapes; (b) Run 7, ice formations showing linkage of individual tube rows due to ice bridging; (c) Run 9, upper two rows linked due to ice bridging

the tubes may contribute to reduce the K_{fc} values, the increased flow velocity down the narrowed fluid "channels" formed by the linked tube-bank rows at higher levels of Θ, and the concurrent rise in convective heat transfer along those surfaces, are believed to be sufficient to elevate the K_{fc} values above those of the nonfreezing baseline without ice formations.

A statistical analysis of the in-line experimental data was also performed. All data points, including those that exhibited ice bridging between adjacent tubes, were included in the analysis. The correlation that fits the in-line tube data is as follows:

$$K_{fc} = 1.8784 \times \mathrm{Re}_f^{0.270} \times \Theta^{0.215} \tag{9}$$

This equation is plotted in Figure 12 for a range of five Θ values and shows fair to good agreement, similar to the staggered case, with the experimental data ($R^2 = 0.92$). Comparing the Θ-parameter exponent for the in-line tube bank with ice-formation correlation, 0.215 (Equation 9), with that of the staggered tube bank with ice formation, 0.277 (Equation 8), clearly shows that the in-line tube-bank heat transfer is less sensitive to Θ variation as compared to the staggered configuration.

Conclusions

A total of 63 steady-state forced-convection ice-on-tube experiments were conducted using both a 16-tube staggered and a 16-tube in-line bank arrangement. The two arrangements behaved similarly in performance, yet differed in the magnitude of their ability to function as effective heat exchangers. Although icing of both tube-bank arrangements involving small Θ was found to be detrimental to the overall tube-bank heat transfer rate, experiments having larger ice buildup on the tubes (higher Θ) were found to increase the heat transfer capability of both arrangements to beyond that of a similar-geometry, nonicing tube bank at the same test Reynolds number. Ice bridging, which was found to seriously affect the heat transfer rate through the staggered tube-bank arrangement, occurred more often, but had less impact on the in-line tube bank and was caused by the presumed tube "shadowing" effect. Finally, correlations for both in-line and staggered tube-bank arrangements were developed for future use in ice-on-tube phase-change design studies.

Acknowledgments

This work was supported by the National Science Foundation under Grant CTS-90936312. The first author also gratefully acknowledges support provided by the General Motors Graduate Research Fellowship Program.

References

Cheng, K. C., Inaba, H., and Gilpin, R. R. 1981. An experimental investigation of ice formation around an isothermally cooled cylinder in crossflow. *ASME J. Heat Transfer*, **103**, 733–737

Cheung, F. B. and Epstein, M. 1984. Solidification and melting in fluid flow. In *Advances in Transport Processes*, Vol. 3, A. S. Majumdar and R. A. Mashelkar (eds.). Wiley Eastern, New Delhi, 35–117

Gilpin, R. R., Hirata, T., and Cheng, K. C. 1980. Wave formation and heat transfer at an ice–water interface in the presence of a turbulent flow. *J. Fluid Mech.*, **99**(3), 619–640

Hirata, T., Gilpin, R. R., Cheng, K. C., and Gates, E. M. 1979. The steady state ice layer profile on a constant temperature plate in a forced convection flow—II. The transition and turbulent regimes. *Int. J. Heat Mass Transfer*, **22**, 1435–1443

Hirata, T. and Matsui, H. 1990. Ice formation and heat transfer with water flow around isothermally cooled cylinders arranged in a line. *ASME J. Heat Transfer*, **112**, 707–713

Hirata, T. and Matsui, H. 1992. Freezing and thawing heat transfer with water flow around isothermally cooled cylinders in staggered and aligned arrangements. *ASME J. Heat Transfer*, **114**, 681–687

Lock, G. S. H. and Kaiser, T. M. V. 1985. Icing on submerged tubes: a study of occlusion. *Int. J. Heat Mass Transfer*, **28**(9), 1689–1698

Moffat, R. J. 1988. Describing the uncertainties in experimental results. *Exp. Thermal Fluid Sci.*, **1**, 3–17

Okada, M., Katayama, K., Terasaki, K., Akimoto, M., and Mabune, K. 1978. Freezing around a cooled pipe in crossflow. *JSME*, **21**(160), 1514–1520

Okada, M., Goto, K., and Nakamura, S. 1987. *Proc. 65th National Conference of JSME* (in Japanese) (No. 870-4), 304–305

Torikoshi, K., Nakazawa, Y., and Yamashita, H. 1990. An experimental study of formation and melting of ice about horizontal tubes. *ASME HTD*, **143**, 57–63

Torikoshi, K. and Nakazawa, Y. 1992. An experimental study of formation and melting of ice around horizontal tubes: influence of tube array on ice formation and melting characteristics. *ASME HTD*, **205**, 19–25

Zukauskas, A. and Ulinskas, R. 1988. *Heat Transfer in Tube Banks in Crossflow*. Hemisphere, New York